

The potential of magnetic nanocluster and dual-functional protein-based strategy for noninvasive detection of HBV surface antibodies†

Hengyao Hu,^{‡a} Hao Yang,^{‡a} Ding Li,^b Kan Wang,^a Jing Ruan,^a Xueqing Zhang,^a Jun Chen,^a Chenchen Bao,^a Jiajia Ji,^a Donglu Shi^{ac} and Daxiang Cui^{*a}

Received 15th July 2010, Accepted 20th October 2010

DOI: 10.1039/c0an00517g

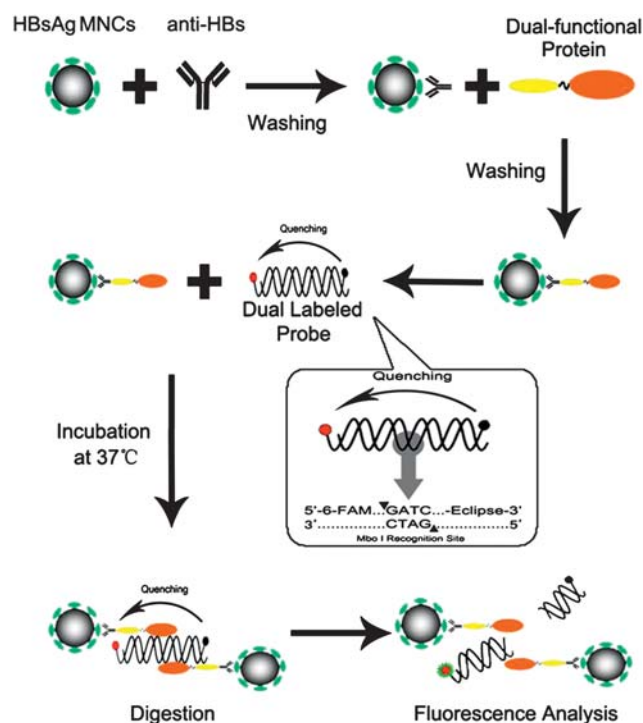
Magnetic nanoclusters (MNCs) were synthesized in a one-pot process, carboxylic MNCs and dual-functional protein were prepared and used to capture hepatitis B virus surface antibodies (anti-HBs) in simulated diseased oral mucosal transudate (OMT) samples. The specific substrate of dual-functional protein, dual-labeled double-stranded DNA molecules, based on Fluorescence Resonance Energy Transfer (FRET), was used to amplify the detection signal and the detection limit of 0.1 ng mL⁻¹ of anti-HBs monoclonal antibodies was achieved. Combination MNCs with dual-functional protein enables the noninvasive detection of hepatitis B virus (HBV) surface antibodies in OMT samples, showing promise as a diagnostic tool for the OMT diagnosis of infectious diseases with sensitive, specific and facile capabilities.

With the rapid progress in nanotechnology, a variety of nano-materials have been developed for biomedical applications.^{1,2} Magnetic nanoparticles, as a promising candidate, exhibit many unique properties that can be used in medical diagnostics and therapeutics. Among those properties, magnetic manipulation based on an external magnetic field provides remarkable advantages for a wide range of applications such as detection, purification, toxin decorporation, and drug delivery.³⁻⁸ For example, magnetic nanoparticles have been applied to hepatitis B virus (HBV) surface antigen detection by immunovoltammetry and HBV DNA analysis by non-faradic electrochemical impedance spectroscopy.^{9,10}

Fluorescence Resonance Energy Transfer (FRET) is a photo-physical process by which energy is transferred from a fluorophore in an excited state to another one.¹¹ FRET will occur on the condition that two fluorophores are in close proximity and the emission spectrum of one fluorophore overlaps the excitation spectrum of the other, which has been explored for medical diagnostic applications. For example, Real-Time Polymerase Chain Reaction (RT-PCR), the most popular tool in quantification of gene expression, combines the

amplification effect of Polymerase Chain Reaction with FRET process and plays an important role in genetic analysis.^{12,13} The reason for its popularity depends on its unique exponential amplification of signal which produces considerably high sensitivity reported to reach several copies of target sequence.¹⁴ Although RT-PCR was originally introduced as an analytical tool for nucleic acid, its exponential amplification power attracted a lot of attention in applying similar technology to detect other biomolecules such as proteins or small molecule antigens. This technology is called quantitative immuno-PCR (qIPCR) with a 10- to 1,000-fold increase in sensitivity compared with Enzyme-Linked Immunosorbent Assay (ELISA).¹⁵ However, its shortcomings include needing too many assay steps, and too long an assay time.

In our laboratory, we have successfully developed several fluorescence-based methods for biomedical detection.¹⁶⁻¹⁸ However, all those methods almost depend on direct analysis of difference of the fixed amount of fluorescent signal or fluorescent intensity on captured probe, and do not have any means of signal amplification. Herein, we report a novel antibody detection strategy based on magnetic nanoclusters (MNCs) and dual-functional protein shown in Scheme 1. In this strategy, recombinant Hepatitis B surface antigens



Scheme 1 Schematic diagram of OMT detection.

^aDepartment of Bio-nano-Science and Engineering, National Key Laboratory of Nanol/Micro Fabrication Technology, Key Laboratory for Thin Film and Microfabrication of Ministry of Education, Institute of Micro-Nano Science and Technology, Shanghai Jiao Tong University, 800 Dongchuan Road, Shanghai, 200240, P.R. China. E-mail: dxcui@sjtu.edu.cn

^bCenter of biological diagnosis and therapy, No. 261 Hospital of PLA, Beijing, 100094, P.R. China

^cDepartment of Chemical and Materials Engineering, University of Cincinnati, Cincinnati, OH, 45221-0012, USA

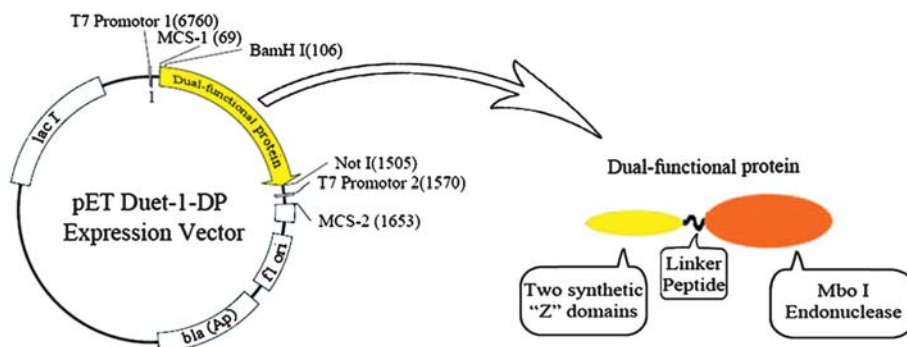
† Electronic supplementary information (ESI) available: Further experimental procedure information and results. See DOI: 10.1039/c0an00517g

‡ Hengyao Hu and Hao Yang are equal contributors to this work.

(HBsAg) are coupled with MNCs as capture probes for Hepatitis B surface antibodies (anti-HBs) in Oral Mucosal Transudate (OMT) samples. Then the secondary antibodies, which are dual-functional protein, bind to the captured anti-HBs. Dual-labeled double chain nucleic acid substrates are finally added into this reaction system for detection of recovered fluorescence caused by specific digestion of the dual-functional protein. The design of dual-functional protein is illustrated in Scheme 2. The gene coding two "Z" domain (binding Immunoglobulin G Fc fraction), linker (avoiding structural and functional interference between "Z" domain and Mbo I endonuclease), and Mbo I endonuclease gene is cloned into pET Duet-1 vector and expressed in bacteria. The resultant fusion protein

possesses two different functions: one is to bind Immunoglobulin G, and the other is to digest double chain DNA at a specific site. The proof-of-principle demonstration described herein highly suggests that this strategy has great potential in applications such as ultra-sensitive detection of bacteria or virus antibodies in OMT samples.

Firstly, the magnetite nanoparticles were prepared by using a traditional solvothermal reaction.¹⁹⁻²¹ Then, magnetic nanoclusters of 172 nm or so in diameter (see Figure S2†) were synthesized when the concentration of $\text{FeCl}_3 \cdot 6\text{H}_2\text{O}$, citrate acid and polyvinyl alcohol (PVA) was respectively 0.1M, 0.001M, and 0.05M. The as-prepared MNCs are shown in Fig. 1 A and C, which demonstrate that the clusters are nearly spherical and uniform in size. The as-prepared



Scheme 2 Schematic diagram of dual-functional protein.

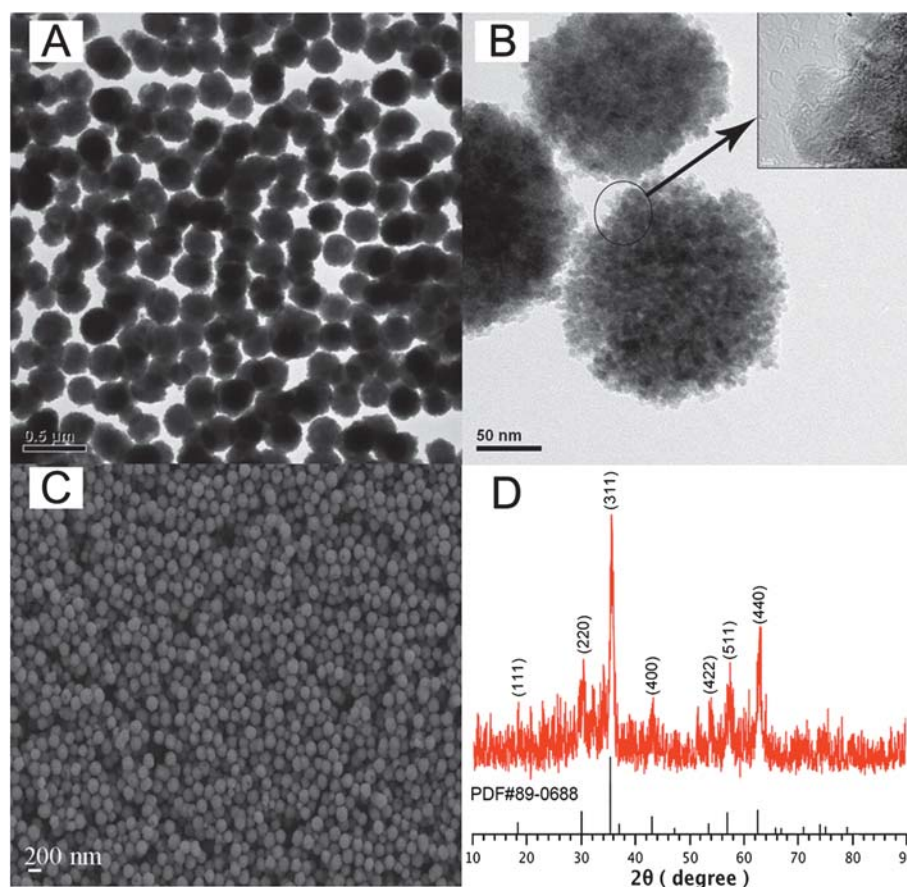


Fig. 1 Characterization of MNCs synthesized in one-pot manner: (A) TEM; (B) HRTEM; (C) SEM; (D) XRD diffraction patterns.

MNCs were very stable, no aggregation was observed. Fig. 1 B shows the precise structure of the MNCs and the high-resolution transmission electron microscopy (HRTEM) image indicates that each cluster is composed of many nanocrystals of about 3–8 nm. The atomic lattice fringes indicate the crystalline nature of the nanocrystals. The power X-ray diffraction (XRD) pattern also shows that the as-prepared magnetite nanoclusters have an inverse spinel type structure (Fig. 1 D). The position and relative intensity of most peaks match well with standard Fe_3O_4 powder diffraction data (JCPDS89-0688), indicating that the magnetite nanocrystals in nanoclusters are crystalline. Fourier transform infrared (FT-IR) spectra of the MNCs obtained with citric acid and PVA indicate characteristic absorption peaks at 1630 and 1384 cm^{-1} associated with the C=O symmetric and antisymmetric stretching respectively, further showing the existence of carboxyl groups (Fig. 2 A).²² The absorption peaks at 3427 and 1055–1114 cm^{-1} associated with the O–H symmetric and C–O–C antisymmetric stretching respectively indicate the existence of PEG on the surface of magnetite nanoclusters. Thermogravimetric analysis (TGA) and differential scanning calorimetry (DSC) in N_2 of magnetite nanoclusters show a large weight loss of about 25.5 wt% at around 300 °C for the 200 nm MNCs (Fig. 2 B). It implies that as-synthesized MNCs include considerable amount of organic species, which might be polyethylene glycol (PEG) and citric acid. Due to the

electrostatic repulsion and steric hindrance effects, the magnetite nanoclusters can be easily dispersed in water and alcohol to form a stable dispersion, which is very stable within almost three months, no aggregation is observed.

The magnetic properties of as-synthesized nanoclusters indicate that the nanoclusters exhibit superparamagnetic behavior with a saturation moment of 43 emu g^{-1} at 300 K, as shown in Fig. 3. Although the average size of nanoclusters is larger than that of the single domain of superparamagnetism for magnetite (30 nm) according to the previous reports, the grain sizes of magnetite nanocrystals (3–8 nm) in nanoclusters are smaller than those of the single domain magnetite.²³ Therefore the nanoclusters exhibit superparamagnetism at room temperature and can be used as an ideal candidate for biomedical applications. The coupling efficiency of HBsAg on MNCs was calculated by this equation: Coupling efficiency = $(\text{OD}_{280} \text{ of pre-coupling} - \text{OD}_{280} \text{ of post-coupling}) / \text{OD}_{280} \text{ of pre-coupling}$. Approximate 11% of coupling efficiency was obtained, which was equal to about 110 μg HBsAg per mg MNCs, while few HBV surface antigens were coupled on MNCs in control without 1-ethyl-3-(3-dimethylaminopropyl)carbodiimide hydrochloride (EDC).

Secondly, the dual-functional protein was prepared. In recent years, there have been several interesting fusion proteins ferrying two distinct functions (antibody and enzyme or toxin) that have been developed for biological analysis and biopharmaceuticals.^{22,24–26} We adopted a similar strategy in this work. With the aim of developing a specific probe that is free of coupling process and capable of amplification of detection signal, we designed a novel fusion protein with capability of both binding Immunoglobulin G Fc fraction and Mbo I endonuclease. According to the idea shown in Scheme 2, the coding sequence of “ZZ” domain in cloning vector pEZZ18 (Genbank Accession: M74186, from nt 2435 to nt 2911), 25-amino acid of linker peptide (ANSSSVEACGRTRSTLEDPRVPVAT) and Mbo I endonuclease (Genbank Accession: D13968, from nt 1026 to nt 1865) was synthesized in succession and cloned into MCS-1 of pET Duet-1. The designed fusion protein comprises 477 amino acid residues and the theoretical molecular weight is 53.81 kilodaltons. In addition, 885 nucleotides of Mbo I methyltransferase A coding sequence (Genbank Accession: D13968, from nt 137 to nt 1021) was synthesized and cloned into MCS-2 of the same pET Duet-1 mentioned above in order to prevent the expressed Mbo I from

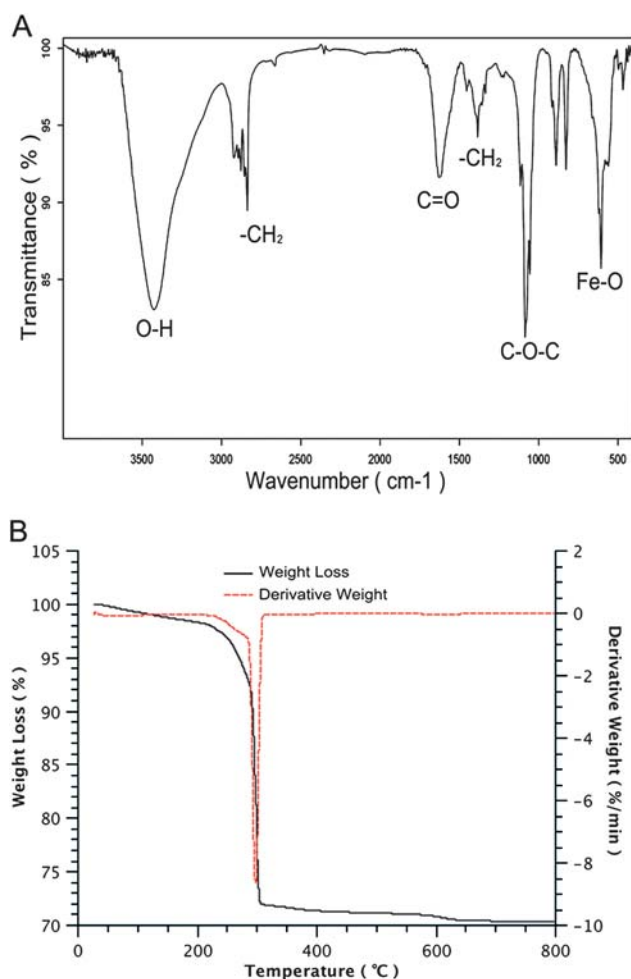


Fig. 2 Characterization of functional groups of MNCs: (A) FT-IR spectra of MNCs; (B) Thermogravimetric curves of MNCs.

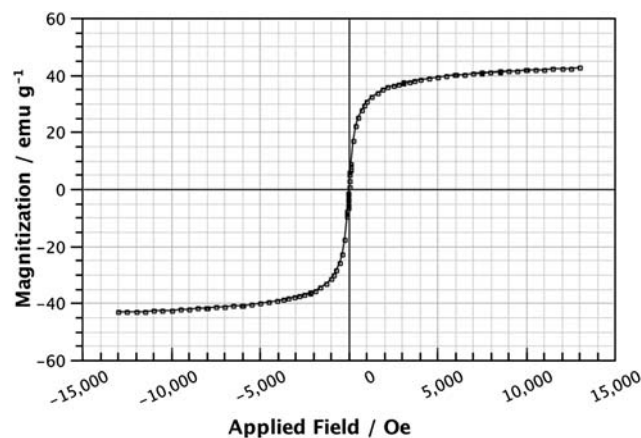


Fig. 3 Magnetization curves of CMNCs powders measured at 300 K.

digesting nucleic acid of host strain.²⁷ The designed protein weighs 33.77 kilodaltons.

After Isopropyl- β -D-thiogalactopyranoside (IPTG) induction, the designed dual-functional protein and Mbo I methyltransferase A were co-expressed successfully in BL21 (DE3) harboring pET Duet-1 DP expression vector and their molecular weights were consistent with our previous expectation. With the prolonged induction time, the amount of corresponding proteins increased significantly (Fig. 4 A). In addition, the dual-functional protein purified by immuno-affinity column exhibited a single band in SDS-PAGE, which represented a good purity of product as well as specific binding to Immunoglobulin G (Fig. 4 A, lane 6). In Fig. 4 B, there are two clear bands at about 326 bp and 148 bp in lane 2 and 3, the band pattern of digestion by dual-functional protein was identical with that by commercial Mbo I endonuclease.

Thirdly, we confirmed the feasibility of this method based on combination of magnetic nanocluster and dual-functional protein. It is well known that the amounts of target molecules, which are immunoglobulin in our work, are much less in saliva than in serum.^{28–30} This implies that saliva diagnostics require higher sensitive methods over traditional ones commonly used in serum detection. To resolve this problem, we have taken measures from several facets. The first one is to take OMT, but not the whole saliva, as our detection sample. This is due to that fact that two kinds of major immunoglobulins (Immunoglobulin G and Immunoglobulin A) are much richer in OMT than in whole saliva.²⁸ Moreover, OMT is an ultrafiltrate of blood, which reflects the level of Immunoglobulin G in serum.³¹ The second one is to increase the volume of OMT sample for detection. During the assay with Aware™ HIV-1/2 OMT Test kit, only 200 μ L of OMT sample

diluted in sample buffer was used for assay. However, only 1 mL of OMT sample was available in single sampling, an ineffective use of the sample. In our experiments, we efficiently utilized the entire sample by magnetic separation with functionalized MNCs. In this way, the available target molecules were 5 times more in our experiments than in the Aware™ human immunodeficiency virus –1/2 (HIV-1/2) OMT Test kit in theory. With these unique approaches, we designed a special signal amplification system based on dual-functional fusion protein that could digest double-stranded DNA fragments at a specific site. Prolonging reaction time could amplify the detection signal gradually.

The supernatant fluorescence spectra in Fig. 5 shows that the different fluorescence intensities are recovered in assays with a series of anti-HBs concentration. The maximum fluorescence wavelength is at \sim 520 nm. The more the dual-functional protein molecules are bound to anti-HBs on MNCs, the more dual-labeled double chain nucleic acid substrates would be digested. Therefore, more FAM fluorophore molecules (see Figure S1†) would be quenched by Eclipse recovered from FRET (Fig. 6). Although the linear correlation of enzyme digestion in our experiment is not as significant as we expected, from the qualitative point of view, the test results can be clearly differentiated between positive (above 0.1 ng mL⁻¹ anti-HBs monoclonal antibodies in simulated OMT samples) and negative ones after 40 min of reaction (Fig. 6 and Figure S3†). Besides, in order to retain the significant difference between positive and negative

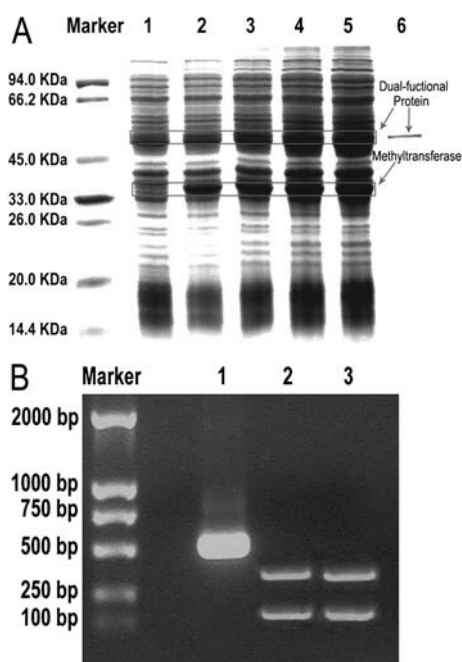


Fig. 4 Characterization of dual-functional protein: (A) SDS-PAGE image of induced dual-functional protein (Lane 1: Not induced; Lane 2: 1 h; Lane 3: 2 h; Lane 4: 3 h; Lane 5: 4 h; Lane 6: purified Dual-functional Protein); (B) Digestion pattern of dual-functional protein and commercial Mbo I endonuclease.

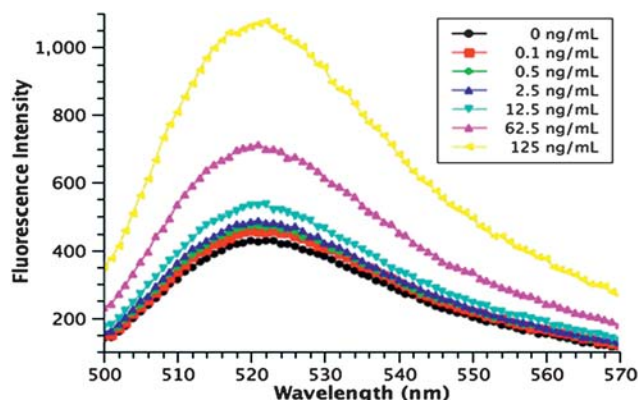


Fig. 5 Fluorescence intensity of different concentrations of anti-HBs in simulated OMT samples.

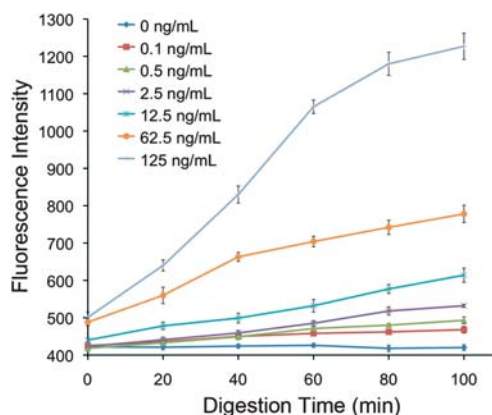


Fig. 6 Signal amplification of detection of simulated OMT samples.

results and cut down the detection time to an acceptable extent, we deliberately set the time of digestion as 1 h, making the total detection time below 2.5 h, which is equal to that of conventional ELISA method. (The test result shown in table S1†).

In summary, we have developed a novel and convenient anti-HBs antibody OMT detection method, which is based on MNCs synthesized in a facile one-pot manner and specially designed dual-functional protein. In this unique approach, MNCs could specifically and rapidly enrich target molecules from OMT samples, and the artificial dual-functional protein could specifically amplify detection signal. The detection limit of our method was 0.1 ng mL⁻¹ of anti-HBs monoclonal antibodies in simulated OMT samples. Furthermore, it should be possible to extend our strategy from this work to other kinds of detection (e.g., antigen, ligand, acceptor) in order to bring its potentiality into full play. One could easily envision its unique signal amplification in future protein analysis. Although there is still lots of work needed to improve the performance of this strategy, activity of artificial enzyme and optimization of digestion reaction for instance, this strategy provides a brand-new idea for protein analysis. Through this work, our strategy provides a good base for the development of commercial OMT detection kit and has great potential in the future application of noninvasive diagnosis in OMT.

Acknowledgements

This work was supported by the National Natural Science Foundation of China (No.20803040), Chinese 973 Project (2010CB933901), 863 Key Project (2007AA022004), New Century Excellent Talent of Ministry of Education of China (NCET-08-0350), Special Infection Diseases Key Project of China (2009ZX10004-311), Shanghai Science and Technology Fund (10XD1406100).

Notes and references

- 1 E. Pierstorff and H. D., *J. Nanosci. Nanotechnol.*, 2007, **7**, 2949–2968.
- 2 Z. Wang, J. Ruan and D. Cui, *Nanoscale Res. Lett.*, 2009, **4**, 593–605.
- 3 X. You, R. He, F. Gao, J. Shao, B. Pan and D. Cui, *Nanotechnology*, 2007, **18**, 035701.
- 4 B. Pan, D. Cui, Y. Sheng, C. S. Ozkan, F. Gao, R. He, Q. Li, P. Xu and T. Huang, *Cancer Res.*, 2007, **67**, 8156–8163.
- 5 R. He, X. You, J. Shao, F. Gao, B. Pan and D. Cui, *Nanotechnology*, 2007, **18**, 315601.
- 6 Q. A. Pankhurst, N. K. T. Thanh, S. K. Jones and J. Dobson, *J. Phys. D: Appl. Phys.*, 2009, **42**, 224001.
- 7 J. Gao, H. Gu and B. Xu, *Acc. Chem. Res.*, 2009, **42**, 1097–1107.
- 8 D. Cui, Y. Han, Z. Li, H. Song, K. Wang, R. He, B. Liu, H. Liu, C. Bao, P. Huang, J. Ruan, F. Gao, H. Yang, H. S. Cho, Q. Ren and D. Shi, *Nano Biomed. Eng.*, 2009, **1**, 94–112.
- 9 C. Qiong, Z. P. Tu and A. L. Liu, *Chin. Chem. Lett.*, 2005, **16**, 1059–1062.
- 10 M. H. Walid, C. Carole, A. Adnane, B. François, L. Didier and J.-R. Nicole, *Sens. Actuators, B*, 2008, **134**, 755–760.
- 11 M. Lorenz and S. Diekmann, *Methods Mol. Biol.*, 2006, **335**, 243–255.
- 12 H. D. VanGuilder, K. E. Vrana and W. M. Freeman, *BioTechniques*, 2008, **44**, 619–626.
- 13 D. Cui, Q. Li, P. Huang, K. Wang, Y. Kong, H. Zhang, X. You, R. He, H. Song, J. Wang, C. Bao, T. Asahi, F. Gao and T. Osaka, *Nano Biomed. Eng.*, 2010, **2**, 45–55.
- 14 M. Burns and H. Valdivia, *Eur. Food Res. Technol.*, 2007, **226**, 1438–2377.
- 15 C. M. Niemeyer, M. Adler and R. Wacker, *Nat. Protoc.*, 2007, **2**, 1918–1930.
- 16 L. Ao, F. Gao, B. Pan, R. He and D. Cui, *Anal. Chem.*, 2006, **78**, 1104–1106.
- 17 D. Cui, B. Pan, H. Zhang, F. Gao, R. Wu, J. Wang, R. He and T. Asahi, *Anal. Chem.*, 2008, **80**, 7996–8001.
- 18 H. Yang, Q. Guo, R. He, D. Li, X. Zhang, C. Bao, H. Hu and D. Cui, *Nanoscale Res. Lett.*, 2009, **4**, 1469–1474.
- 19 J. Liu, Z. Sun, Y. Deng, Y. Zou, C. Li, X. Guo, L. Xiong, Y. Gao, F. Li and D. Zhao, *Angew. Chem., Int. Ed.*, 2009, **48**, 5875–5879.
- 20 H. Deng, X. Li, Q. Peng, X. Wang, J. Chen and Y. Li, *Angew. Chem.*, 2005, **117**, 2842–2845.
- 21 M. Carmen, O. Bomati-Miguel, P. Morales, C. Serna and S. Veintemillas-Verdaguer, *J. Magn. Magn. Mater.*, 2005, **293**, 20–27.
- 22 D. Rau, K. Kramer and B. Hock, *J. Immunoassay Immunochem.*, 2002, **23**, 129–143.
- 23 C. Cheng, Y. Wen, X. Xu and H. Gu, *J. Mater. Chem.*, 2009, **19**, 8782–8788.
- 24 R. Hakim and I. Benhar, *mAbs*, 2009, **1**, 281–287.
- 25 X. Liu, H. Wang, Y. Liang, J. Yang, H. Zhang, H. Lei, Y. Shen and Y. Sun, *Mol. Biotechnol.*, 2010, DOI: 10.1007/s12033-010-9240-2.
- 26 V. Pingoud, A. Sudina, H. Geyer, J. M. Bujnicki, R. Lurz, G. Lüder, R. Morgan, E. Kubareva and A. Pingoud, *J. Biol. Chem.*, 2005, **280**, 4289–4298.
- 27 D. Malamud, *Am. J. Med.*, 1997, **102**, 9–14.
- 28 D. T. Wong, *J. Am. Dent. Assoc.*, 2006, **137**, 313–321.
- 29 P. A. Maple, I. Simms, G. Kafatos, M. Solomou and K. Fenton, *Eur. J. Clin. Microbiol. Infect. Dis.*, 2006, **25**, 743–749.
- 30 L. F. Hofman, *J. Nutr.*, 2001, **131**, 1621S–1625S.
- 31 S. O. Cameron and W. F. Carman, *J. Clin. Virol.*, 2005, **34**, S22–28.